

Christoffel equation in the polarization variables

Vladimir Grechka¹

¹*Borehole Seismic, LLC*

(Dated: July 25, 2019)

We formulate the classic Christoffel equation in the polarization variables and solve it for the slowness vectors of plane waves corresponding to a given unit polarization vector. Our analysis shows that, unless the equation degenerates and yields an infinite number of different slowness vectors, the finite nonzero number of its legitimate solutions varies from 1 to 4. Also we find a subset of triclinic solids in which the polarization field can have holes; there exist finite-size solid angles of polarization directions unattainable to any plane wave.

PACS numbers: 81.05.Xj, 91.30.-f

I. INTRODUCTION

The Christoffel¹ equation governs the propagation of plane waves in homogeneous anisotropic media. A textbook approach²⁻⁴ to solving it consists in specifying the unit wavefront normal vector \mathbf{n} , constructing the symmetric, positive-definite Christoffel tensor $\mathbf{\Gamma}$, and computing solution to the ensuing eigenvalue-eigenvector problem — the phase velocities V and the unit polarization vectors \mathbf{U} of three body waves propagating along the selected wavefront direction \mathbf{n} . If that \mathbf{n} is not a singularity, all three vectors \mathbf{U} are unique; alternatively, if \mathbf{n} happens to be a singularity, some of vectors \mathbf{U} or all of them are nonunique.

The introduction of the slowness vector $\mathbf{p} = \mathbf{n}/V$ translates the uniqueness of \mathbf{U} into uniqueness of the corresponding group-velocity vector \mathbf{g} ^{2,3}. Its normalized version, the ray vector $\mathbf{r} \equiv \mathbf{g}/|\mathbf{g}|$, emerges in two-point ray-tracing⁵ as a natural variable for the description of velocities and polarizations of high-frequency waves, their number, for a given ray direction \mathbf{r} in a homogeneous anisotropic medium, ranging from three to nineteen⁶. Thus, all properties of plane waves propagating in a homogeneous anisotropic medium can be computed as functions of either unit vector \mathbf{n} or \mathbf{r} .

This paper discusses a similar computation for a unit polarization vector \mathbf{U} selected as such a primary variable. A physical experiment encouraging the understanding of waves parameterized by \mathbf{U} would be a record of wave motion by a single three-component sensor placed in a homogeneous elastic solid. If such a sensor is located sufficiently far from a source, it would record vectors \mathbf{U} of individual body waves. Then one might wonder what kind of information about the local velocities or slownesses of these waves could be extracted from the measured direction of \mathbf{U} and the knowledge of the medium — the inquiry pursued here.

II. THEORY

An obvious point of departure for our investigation is the Christoffel equation²⁻⁴

$$\mathbf{\Gamma}(\mathbf{p}) \cdot \mathbf{U} = U, \quad (1)$$

where \mathbf{p} is the slowness vector, \mathbf{U} is the unit polarization vector,

$$\mathbf{\Gamma}(\mathbf{p}) \equiv \mathbf{p} \cdot \mathbf{c} \cdot \mathbf{p} \quad (2)$$

is the second-rank 3×3 positive-definite Christoffel tensor or matrix, and \mathbf{c} is the fourth-rank $3 \times 3 \times 3 \times 3$ density-normalized stiffness tensor. We wish to solve equation 1 for \mathbf{p} given the knowledge of \mathbf{U} and \mathbf{c} .

One can immediately observe that function $\mathbf{p} = \mathbf{p}(\mathbf{U})$ is not necessarily unique. A simple example, exposing its nonuniqueness, is supplied by SH-waves propagating in the vertical $[\mathbf{x}_1, \mathbf{x}_3]$ plane of a purely isotropic medium, the waves that have identical polarization vectors $\mathbf{U}^{\text{SH}} = [0, 1, 0]$ for any in-plane slowness vector $\mathbf{p}^{\text{SH}} = [p_1^{\text{SH}}, 0, p_3^{\text{SH}}]$. Still, the presented exception does not negate the fact that equation 1 is a system of three quadratic equations for the three components of slowness vector $\mathbf{p} = [p_1, p_2, p_3]$. When non-degenerative, system 1 has a finite number of roots, and Bézout's theorem⁷ equates their maximum number to the product of degrees of individual equations, that is, $2 \times 2 \times 2 = 8$. Also because a real-valued root \mathbf{p} of system 1 is always accompanied by its centrally symmetric opposite $-\mathbf{p}$,

The maximum number of distinct (that is, non-centrally symmetric) real-valued roots of non-degenerative system 1 is equal to 4.

Once these slowness roots are found, the corresponding phase and group velocities are given by²⁻⁴

$$V = \frac{1}{|\mathbf{p}|} \quad (3)$$

and

$$\mathbf{g} = \mathbf{\Gamma}(\mathbf{U}) \cdot \mathbf{p}. \quad (4)$$

III. ISOTROPY

The analysis of system 1, shorthand as the $\mathbf{p}(\mathbf{U})$ problem, is easiest in isotropic media, where the system does not even need to be solved to understand the properties of its solutions. Indeed, because $\mathbf{p}^P \parallel \mathbf{U}^P$ for the P-waves and $\mathbf{p}^S \perp \mathbf{U}^S$ for the S-waves, a given vector \mathbf{U} uniquely constrains \mathbf{p}^P and yields infinitely many slowness vectors \mathbf{p}^S , confined to the plane orthogonal to \mathbf{U} .

Let us derive this simple result from equation 1. Because all directions are equivalent in isotropic media, the coordinate axis \mathbf{x}_1 can be oriented along our polarization vector \mathbf{U} that becomes $\mathbf{U} = [1, 0, 0]$ in the new coordinate frame. Then, the substitution of that \mathbf{U} in system 1, written for isotropic stiffness tensor \mathbf{c} expressed in terms of Lamé constants λ and μ , reduces the system to

$$\begin{cases} (\lambda + 2\mu) p_1^2 + \mu (p_2^2 + p_3^2) = 1, & (5a) \\ (\lambda + \mu) p_1 p_2 = 0, & (5b) \\ (\lambda + \mu) p_1 p_3 = 0, & (5c) \end{cases}$$

implying two possible scenarios.

1. If equations 5b and 5c are satisfied by setting $p_2 = p_3 = 0$, equation 5a yields a uniquely defined direction of the centrally symmetric P-wave slowness vector

$$\mathbf{p}^P = \left[\pm \frac{1}{\sqrt{\lambda + 2\mu}}, 0, 0 \right]. \quad (6)$$

2. Alternatively, if both equations 5b and 5c are satisfied by setting $p_1 = 0$, equation 5a, relating the two remaining unknowns p_2 and p_3 , describes a circle in the $[p_2, p_3]$ plane, resulting in the S-wave slowness vectors

$$\mathbf{p}^S \equiv \mathbf{p}^S(\varphi) = \left[0, \frac{\sin \varphi}{\sqrt{\mu}}, \frac{\cos \varphi}{\sqrt{\mu}} \right] \forall \varphi \quad (7)$$

and confirming the fact that the shear-wave slowness vector \mathbf{p}^S cannot be uniquely derived from polarization vector \mathbf{U} .

IV. VERTICAL TRANSVERSE ISOTROPY

The $\mathbf{p}(\mathbf{U})$ problem in vertically transversely isotropic (VTI) media offers much more variety than that in just examined isotropic media, entailing several intriguing special cases. We will analyze them as they get discovered, starting from the general scenario, in which all three components of a given polarization vector \mathbf{U} are nonzero, and system 1 reads^{2,8}

$$\begin{pmatrix} c_{11} p_1^2 + c_{66} p_2^2 + c_{55} p_3^2 & (c_{11} - c_{66}) p_1 p_2 & (c_{13} + c_{55}) p_1 p_3 \\ (c_{11} - c_{66}) p_1 p_2 & c_{66} p_1^2 + c_{11} p_2^2 + c_{55} p_3^2 & (c_{13} + c_{55}) p_2 p_3 \\ (c_{13} + c_{55}) p_1 p_3 & (c_{13} + c_{55}) p_2 p_3 & c_{55} (p_1^2 + p_2^2) + c_{33} p_3^2 \end{pmatrix} \cdot \begin{bmatrix} U_1 \\ U_2 \\ U_3 \end{bmatrix} = \begin{bmatrix} U_1 \\ U_2 \\ U_3 \end{bmatrix}, \quad (8)$$

where c_{ij} ($i, j = 1, \dots, 6$) are the density normalized stiffness coefficients in Voigt notation.

Mere inspection of matrix $\mathbf{\Gamma}(\mathbf{p})$ in the left side of system 8 reveals a special case: if $c_{13} = -c_{55}$ (unlikely for natural materials but mathematically possible), one eigenvector \mathbf{U} of such a $\mathbf{\Gamma}(\mathbf{p})$ is always vertical, whereas two other eigenvectors are always horizontal regardless of the value of \mathbf{p} . Although superficial reaction to this observation might be that equations 8 become incompatible for an arbitrary direction of \mathbf{U} , a more careful investigation, presented below, is warranted.

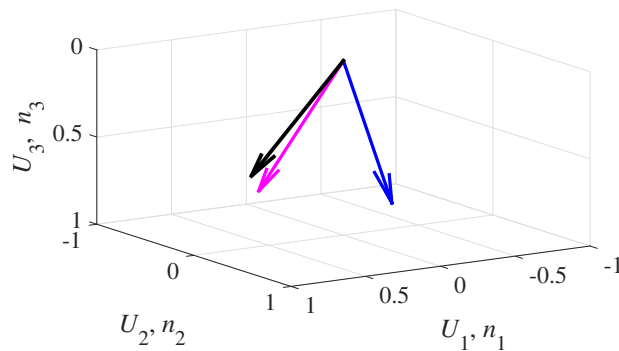


FIG. 1: Input polarization vector $\mathbf{U} = [0.806, 0.293, 0.515]$ (the black arrow) and wavefront normals of the P- (the magenta arrow) and SV-waves (the blue arrow) calculated in VTI model 9 by solving equations 8.

When $c_{13} \neq -c_{55}$, as typically expected in VTI solids, matrix $\mathbf{\Gamma}(\mathbf{p})$ has one horizontal eigenvector $\mathbf{U} = \mathbf{U}^{\text{SH}}$ corresponding to the SH-wave. Hence, unless $U_3 = 0$ — another special case — the SH-wave slowness vector $\mathbf{p} = \mathbf{p}^{\text{SH}}$ cannot be obtained by solving equations 8 for the components of \mathbf{p} . Consequently, equations 8 can have two real-valued roots that describe slowness vectors of the P- and SV-waves for an arbitrary polarization vector \mathbf{U} .

Figure 1, computed for a VTI stiffness matrix (in arbitrary units of velocity squared, as well as other stiffness matrixes below)

$$\mathbf{c} = \begin{pmatrix} 22.4 & 17.6 & 9.5 & 0 & 0 & 0 \\ & 22.4 & 9.5 & 0 & 0 & 0 \\ & & 16 & 0 & 0 & 0 \\ & \text{SYM} & & 4 & 0 & 0 \\ & & & & 4 & 0 \\ & & & & & 2.4 \end{pmatrix}, \quad (9)$$

with “SYM” denoting the symmetric part of \mathbf{c} , illustrates this arrangement. Equations 8 have the real-valued slowness solutions $\mathbf{p} = \mathbf{p}^{\text{P}}$ and $\mathbf{p} = \mathbf{p}^{\text{SV}}$, and Figure 1 displays the corresponding wavefront normals $\mathbf{n} = \mathbf{p}/|\mathbf{p}|$. The P-wave normal \mathbf{n}^{P} (magenta) is close to the polarization vector \mathbf{U} (black), whereas the SV normal \mathbf{n}^{SV} (blue) is approximately orthogonal to it.

The two slowness solutions shown in Figure 1, however, do not exhaust all the possibilities. If a VTI model possesses intersection singularities⁹ \mathbf{n}^s , polarization vector $\mathbf{U}(\mathbf{n}^s)$ at a singularity might happen to be equal to an input vector \mathbf{U} , making the singular slowness vector \mathbf{p}^s a part of real-valued solution of equations 8; also because a vertical plane containing an arbitrary vector \mathbf{U} is a symmetry plane of a VTI medium, singular solutions \mathbf{p}^s of equations 8 always come in non-centrally symmetric pairs.

To investigate this scenario, we increase the stiffness coefficient c_{66} in matrix 9 to make $c_{66} > c_{55}$ and create an intersection singularity in VTI model

$$\mathbf{c} = \begin{pmatrix} 22.4 & 11.2 & 9.5 & 0 & 0 & 0 \\ & 22.4 & 9.5 & 0 & 0 & 0 \\ & & 16 & 0 & 0 & 0 \\ & \text{SYM} & & 4 & 0 & 0 \\ & & & & 4 & 0 \\ & & & & & 5.6 \end{pmatrix} \quad (10)$$

at $\mathbf{n}^s = [0.656, 0, 0.764]$ in the $[\mathbf{x}_1, \mathbf{x}_3]$ plane. Figure 2 presents the obtained wavefront normals for the same polarization vector $\mathbf{U} = [0.806, 0.293, 0.515]$ (the black arrow) as that in Figure 1. Indeed, the two singular wavefront normals \mathbf{n}^s (the green arrows in Figure 2) have been recovered from equations 8 in addition to \mathbf{n}^{P} (the magenta arrow) and \mathbf{n}^{SV} (the blue arrow).

A. Equality $c_{13} = -c_{55}$

The presented example allows us to understand how to properly treat the special case of equality

$$c_{13} = -c_{55}. \quad (11)$$

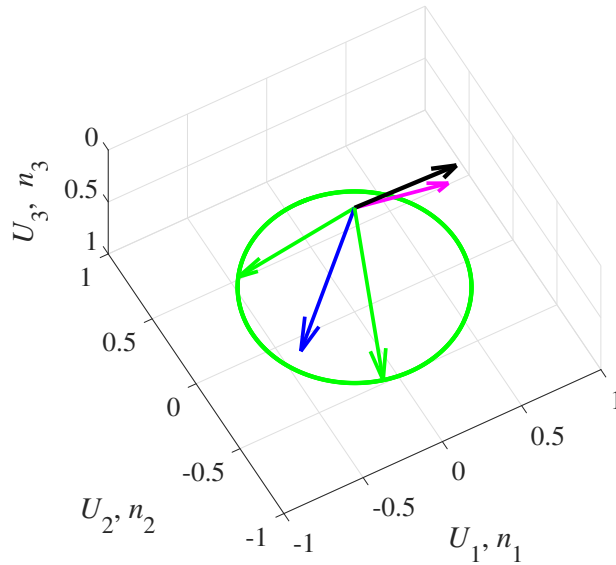


FIG. 2: Same as Figure 1 but for VTI model 10. In addition to wavefront normals of the P- (the magenta arrow) and SV-waves (the blue arrow), solutions of equations 8 contain two singular normals (the green arrows), connected to the green circle that marks the SV-SH wave intersection singularity.

Even though matrix $\mathbf{\Gamma}(\mathbf{p})$ in system 8 does have one vertical and two horizontal eigenvectors, the presence of intersection singularities could make equations 8 compatible for an arbitrary polarization vector \mathbf{U} . To illustrate that, let us impose constraint 11 on VTI stiffness matrix 10, so that it becomes

$$\mathbf{c} = \begin{pmatrix} 22.4 & 11.2 & -4 & 0 & 0 & 0 \\ & 22.4 & -4 & 0 & 0 & 0 \\ & & 16 & 0 & 0 & 0 \\ & \text{SYM} & & 4 & 0 & 0 \\ & & & & 4 & 0 \\ & & & & & 5.6 \end{pmatrix}. \quad (12)$$

Model 12 exhibits two intersection singularities \mathbf{n}^{s1} and \mathbf{n}^{s2} , indicated by the cyan and green arrows in Figure 3a, and two corresponding internal refraction cones, degenerating into the cyan and green straight lines in Figure 3b. The fans of polarization vectors $\mathbf{U}(\mathbf{n}^{s1})$ and $\mathbf{U}(\mathbf{n}^{s2})$ at those singularities contain vectors equal to the input polarization vector $\mathbf{U} = [0.720, 0.262, 0.643]$ (the black arrow in Figure 4). Hence, all four solutions of equations 8 for this vector \mathbf{U} come from the intersection singularities.

Finally, let us investigate two symmetric orientations of vector \mathbf{U} — along the vertical symmetry axis \mathbf{a} and orthogonally to it.

B. Vertical polarization vector

When input polarization vector is vertical, $\mathbf{U} = [0, 0, 1]$, system 8 simplifies to

$$\begin{cases} (c_{13} + c_{55}) p_1 p_3 = 0, & (13a) \\ (c_{13} + c_{55}) p_2 p_3 = 0, & (13b) \\ c_{55} (p_1^2 + p_2^2) + c_{33} p_3^2 = 1 & (13c) \end{cases}$$

and becomes very similar to system 5 examined for isotropic media. Consequently, three types of solutions are possible — two already analyzed in section III and one related to the equality $c_{13} + c_{55} = 0$, whose analog $\lambda + \mu = 0$ is prohibited for isotropy by the elastic stability conditions.

1. When equations 13a and 13b are satisfied by setting $p_1 = p_2 = 0$, equation 13c yields the vertical P-wave slowness vector

$$\mathbf{p}^P = \left[0, 0, \pm \frac{1}{\sqrt{c_{33}}} \right]. \quad (14)$$

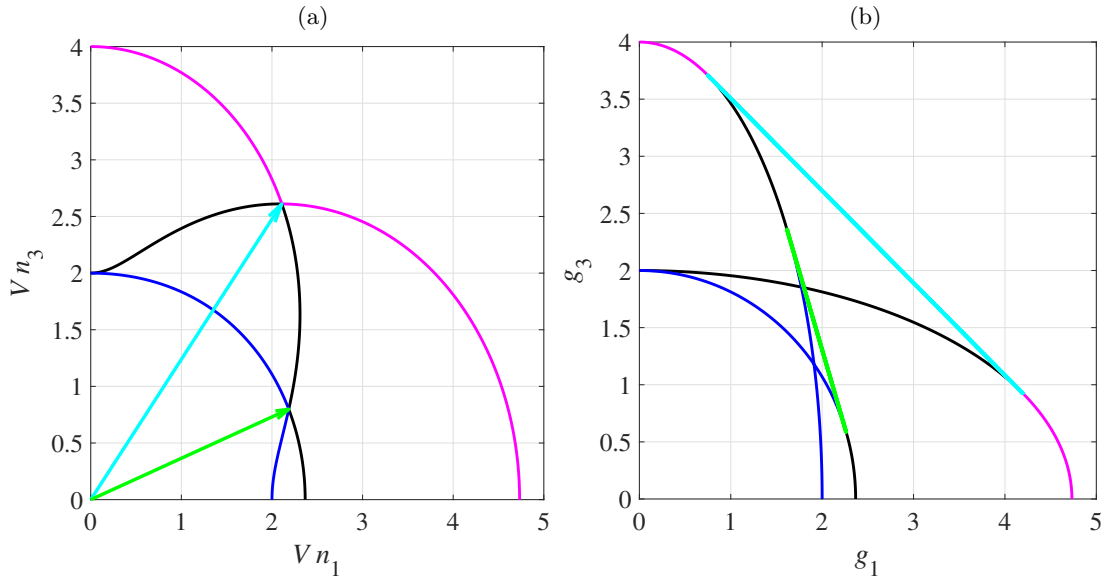


FIG. 3: Quadrants of (a) phase- and (b) group-velocity surfaces of the P- (magenta), S₁- (black) and S₂-waves (blue) in the vertical plane $[\mathbf{x}_1, \mathbf{x}_3]$ of VTI model 12. The directions of two intersection singularities $\mathbf{n}^{s^1} = [0.628, 0, 0.778]$ and $\mathbf{n}^{s^2} = [0.939, 0, 0.343]$ are marked by the cyan and green arrows, respectively, in (a), the corresponding degenerative internal refraction cones — by the cyan and green lines in (b).

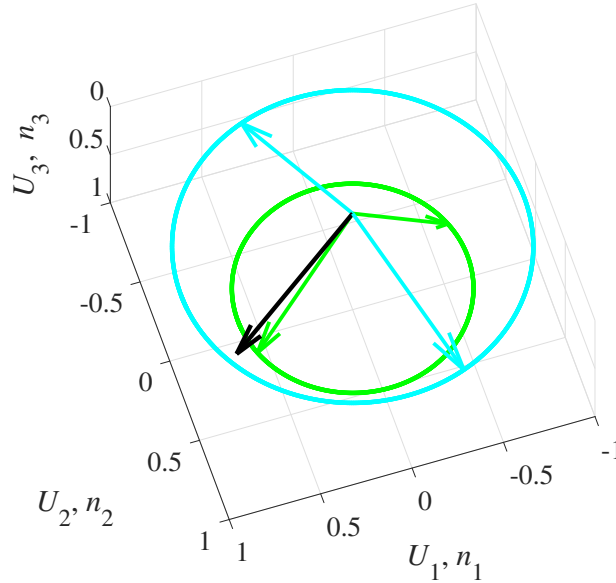


FIG. 4: Same as Figure 2 but for VTI model 12. All four solutions of equations 8, marked by the green and cyan arrows, for polarization vector \mathbf{U} (the black arrow) correspond to intersection singularities indicated by the circles.

- When equations 13a and 13b are satisfied by setting $p_3 = 0$, equation 13c, relating the two remaining unknowns p_1 and p_2 , describes infinitely many shear-wave slowness vectors

$$\mathbf{p}^S \equiv \mathbf{p}^S(\varphi) = \left[\frac{\sin \varphi}{\sqrt{c_{55}}}, \frac{\cos \varphi}{\sqrt{c_{55}}}, 0 \right] \forall \varphi, \quad (15)$$

their ends tracing a circle with radius $1/\sqrt{c_{55}}$ in the $[p_1, p_2]$ plane.

- Finally, when $c_{13} + c_{55} = 0$, equations 13a and 13b are satisfied identically for any slowness vector, whereas equation 13c constraints the components of \mathbf{p} to the surface of a spheroid in the \mathbf{p} -space.

C. Horizontal polarization vector

Because all horizontal directions in a VTI medium are equivalent due to its rotational invariance around the vertical, let us select $\mathbf{U} = [1, 0, 0]$ to simplify our analysis. System 8 then reads

$$\begin{cases} c_{11} p_1^2 + c_{66} p_2^2 + c_{55} p_3^2 = 1, & (16a) \\ (c_{11} - c_{66}) p_1 p_2 = 0, & (16b) \\ (c_{13} + c_{55}) p_1 p_3 = 0, & (16c) \end{cases}$$

implying three possibilities similar to those just discussed for the vertical vector \mathbf{U} .

1. When equations 16b and 16c are satisfied for $p_2 = p_3 = 0$, equation 16a describes the horizontal P-wave slowness vector

$$\mathbf{p}^P = \left[\pm \frac{1}{\sqrt{c_{11}}}, 0, 0 \right]. \quad (17)$$

2. When both equations 16b and 16c are satisfied for $p_1 = 0$, equation 16a yields infinitely many SH-wave slowness vectors

$$\mathbf{p}^{\text{SH}} \equiv \mathbf{p}^{\text{SH}}(\varphi) = \left[0, \frac{\sin \varphi}{\sqrt{c_{66}}}, \frac{\cos \varphi}{\sqrt{c_{55}}} \right] \forall \varphi, \quad (18)$$

their ends placed at an ellipse in the vertical $[p_2, p_3]$ plane.

3. When $c_{13} + c_{55} = 0$ and equation 16b is satisfied for $p_1 = 0$ ($c_{11} - c_{66} > 0$ in accordance with the elastic stability conditions in VTI media), equation 16a describes the slowness vectors given by equation 18. Alternatively, when $c_{13} + c_{55} = 0$ but equation 16b is satisfied for $p_2 = 0$ instead of $p_1 = 0$, equation 16a describes a set of the slowness vectors in the $[p_1, p_3]$ plane,

$$\mathbf{p} = \left[\frac{\sin \varphi}{\sqrt{c_{11}}}, 0, \frac{\cos \varphi}{\sqrt{c_{55}}} \right] \forall \varphi. \quad (19)$$

V. SYMMETRIES LOWER THAN TRANSVERSE ISOTROPY

The analysis of the $\mathbf{p}(\mathbf{U})$ problem presented so far reveals that system 1 can have two, four, or infinitely many slowness solutions for a given polarization vector \mathbf{U} . Clearly, the first two possibilities are realizable in generally anisotropic media because roots of a polynomial system are continuous functions of its coefficients, which are, in turn, continuous functions of the stiffness components. For instance, Figure 5 displays four singularity-unrelated solutions (the magenta and blue arrows) for triclinic model

$$\mathbf{c} = \begin{pmatrix} 50 & 10 & 20 & -5 & 0 & 10 \\ & 50 & 30 & 3 & -5 & 10 \\ & & 50 & 2 & 1 & 0 \\ & \text{SYM} & & 20 & 3 & 5 \\ & & & & 30 & -5 \\ & & & & & 10 \end{pmatrix}. \quad (20)$$

The number of real-valued roots of equations 1 in low-symmetry anisotropic media can be infinite, too. Consider, for example, the vertical polarization vector $\mathbf{U} = [0, 0, 1]$ in an orthorhombic solid described by its generic stiffness matrix. There, equations 1 reduce to a system similar to 13,

$$\begin{cases} (c_{13} + c_{55}) p_1 p_3 = 0, & (21a) \\ (c_{23} + c_{44}) p_2 p_3 = 0, & (21b) \\ c_{55} p_1^2 + c_{44} p_2^2 + c_{33} p_3^2 = 1, & (21c) \end{cases}$$

and because equations 21a and 21b are simultaneously satisfied at $p_3 = 0$, equation 21c yields an infinite number of slowness vectors

$$\mathbf{p} = \left[\frac{\sin \varphi}{\sqrt{c_{55}}}, \frac{\cos \varphi}{\sqrt{c_{44}}}, 0 \right] \forall \varphi. \quad (22)$$

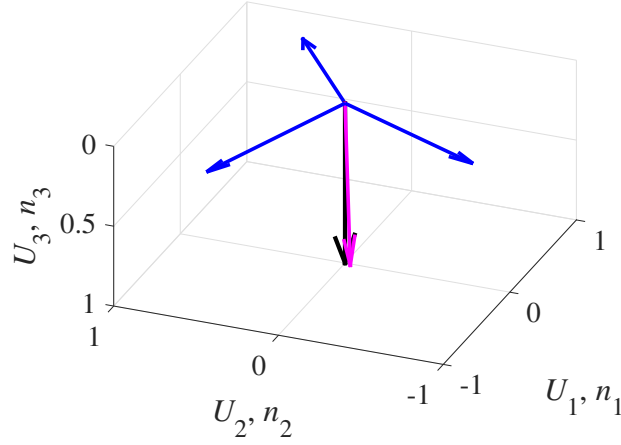


FIG. 5: Same as Figure 1 but for triclinic model 20. The input vertical polarization vector $\mathbf{U} = [0, 0, 1]$ is indicated by the black arrow, the wavefront normals of one P-wave and three S-waves — by the magenta and blue arrows, respectively.

Hence, it remains to investigate whether equations 1 can have zero, one, or three real-valued roots. To address the question pertaining to the existence of one or three real-valued roots in a systematic way, we select a local coordinate frame, in which our input polarization vector $\mathbf{U} = [0, 0, 1]$, and explicitly write system 1 for that \mathbf{U} in triclinic media. The system reads

$$\begin{cases} c_{15} p_1^2 + (c_{14} + c_{56}) p_1 p_2 + (c_{13} + c_{55}) p_1 p_3 + c_{46} p_2^2 \\ + (c_{36} + c_{45}) p_2 p_3 + c_{35} p_3^2 = 0, \end{cases} \quad (23a)$$

$$\begin{cases} c_{56} p_1^2 + (c_{25} + c_{46}) p_1 p_2 + (c_{36} + c_{45}) p_1 p_3 + c_{24} p_2^2 \\ + (c_{23} + c_{44}) p_2 p_3 + c_{34} p_3^2 = 0, \end{cases} \quad (23b)$$

$$\begin{cases} c_{55} p_1^2 + 2 c_{45} p_1 p_2 + 2 c_{35} p_1 p_3 + c_{44} p_2^2 + 2 c_{34} p_2 p_3 + c_{33} p_3^2 = 1, \end{cases} \quad (23c)$$

lending itself to straightforward analysis.

A. One root

If a triclinic model is such that

$$\begin{cases} c_{14} + c_{56} = 0, \end{cases} \quad (24a)$$

$$\begin{cases} c_{13} + c_{55} = 0, \end{cases} \quad (24b)$$

$$\begin{cases} c_{36} + c_{45} = 0, \end{cases} \quad (24c)$$

the cross-terms vanish in equation 23a; if additionally

$$c_{34} = c_{35} = 0, \quad (25)$$

the terms proportional to p_3^2 vanish in both equations 23a or 23b; finally, if the product

$$c_{15} c_{46} > 0, \quad (26)$$

equations 23a and 23b are satisfied for a single pair of real-valued slowness components $p_1 = p_2 = 0$, and equation 23c yields a single centrally symmetric slowness root

$$\mathbf{p}^P = \left[0, 0, \pm \frac{1}{\sqrt{c_{33}}} \right]. \quad (27)$$

B. Three roots

Alternatively, if the opposite of inequality 26 is true,

$$c_{15} c_{46} < 0, \quad (28)$$

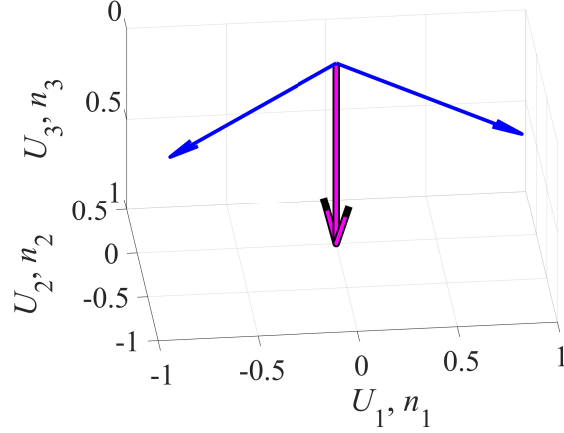


FIG. 6: Same as Figure 5 but for model 30.

equation 23a has two roots, related to each other as

$$\frac{p_1}{p_2} = \pm \sqrt{-\frac{c_{46}}{c_{15}}} \quad (29)$$

and complementing the already discussed root $p_1 = p_2 = 0$. Therefore, system 23 can possess three real-valued roots, as shown in Figure 6 for triclinic stiffness matrix

$$\mathbf{c} = \begin{pmatrix} 50 & 10 & -20 & -5 & 1 & 10 \\ & 50 & 20 & 3 & 6 & 10 \\ & & 50 & 0 & 0 & 2 \\ \text{SYM} & & & 22 & -2 & -5 \\ & & & & 20 & 5 \\ & & & & & 10 \end{pmatrix}. \quad (30)$$

The logic presented for equation 23a would apply to equation 23b when the set of equalities 24 is replaced by

$$\begin{cases} c_{25} + c_{46} = 0, & (31a) \\ c_{36} + c_{45} = 0, & (31b) \\ c_{23} + c_{44} = 0, & (31c) \end{cases}$$

and inequalities 26 or 28 are replaced by

$$c_{56} c_{24} > 0 \quad (32)$$

or

$$c_{56} c_{24} < 0, \quad (33)$$

respectively.

VI. PROHIBITED POLARIZATION DIRECTIONS

An unexpected scenario arises when equations 24 are satisfied, and the signs of three nonzero stiffness coefficients composing the triplet $[c_{15}, c_{35}, c_{46}]$ coincide,

$$\begin{cases} [c_{15}, c_{35}, c_{46}] > 0 \text{ or} & (34a) \\ [c_{15}, c_{35}, c_{46}] < 0. & (34b) \end{cases}$$

Then equation 23a, now in the form

$$c_{15} p_1^2 + c_{46} p_2^2 + c_{35} p_3^2 = 0, \quad (35)$$

has only trivial real-valued solution

$$\mathbf{p} \equiv [p_1, p_2, p_3] = \mathbf{0}, \quad (36)$$

making system 23 incompatible.

As a result, our polarization direction $\mathbf{U} = [0, 0, 1]$ is unattainable to any plane wave regardless of its wavefront normal \mathbf{n} ; and the field of polarization vectors \mathbf{U} develops a *hole* at the vertical. The size of this hole, outlining a solid angle of prohibited polarization directions, is *finite* rather than infinitesimal because a small finite perturbation of order $\varepsilon \ll 1$ of the components of vector $\mathbf{U} = [0, 0, 1]$ replaces equation 35 by

$$c_{15} p_1^2 + c_{46} p_2^2 + c_{35} p_3^2 = \mathcal{O}(\varepsilon) \quad (37)$$

and solution 36 by a real-valued slowness vector that has the length

$$|\mathbf{p}| \sim \mathcal{O}(\sqrt{\varepsilon}), \quad (38)$$

provided that the sign of the right side of equation 37 coincides with that of the stiffnesses in the triplet $[c_{15}, c_{35}, c_{46}]$; otherwise, a solution becomes complex-valued. Clearly, the length of vector \mathbf{p} given by relationship 38 is too small to ensure the compatibility of equations 23.

To illustrate possible sizes of solid angles of prohibited polarization directions, we construct a triclinic model

$$\mathbf{c} = \begin{pmatrix} 50 & 10 & -\mathbf{20} & -\mathbf{5} & \mathbf{1} & 10 \\ & 50 & 20 & 3 & 6 & 10 \\ & & 50 & 0 & \mathbf{4} & \mathbf{2} \\ & \text{SYM} & & 22 & -\mathbf{2} & \mathbf{5} \\ & & & & \mathbf{20} & \mathbf{5} \\ & & & & & 10 \end{pmatrix}, \quad (39)$$

in which the boldface stiffness coefficients obeying conditions 24a, 24b, 24c, and 34a are typeset in black, blue, red, and green, respectively. Next, we solve the Christoffel equation

$$\mathbf{\Gamma}(\mathbf{n}) \cdot \mathbf{U} = V^2 \mathbf{U}, \quad (40)$$

analogous to equation 1, in model 39 for a set of wavefront normals \mathbf{n} spanning the entire unit sphere. The obtained polarization vectors $\mathbf{U}(\mathbf{n})$, displayed in Figure 7, exhibit two finite-size solid angles of prohibited polarization directions, appearing as the white areas.

VII. DISCUSSION AND CONCLUSIONS

The presented analysis allows us to list all the possibilities of describing plane-wave propagation in homogeneous anisotropic media in terms of a single input quantity — the unit vector \mathbf{n} , \mathbf{r} , or \mathbf{U} .

1. Input wavefront normal \mathbf{n} . Solving the Christoffel equation 40 always yields three phase velocities $V_P(\mathbf{n})$, $V_{S1}(\mathbf{n})$, and $V_{S2}(\mathbf{n})$ of the P-, S₁-, and S₂-waves, equal to square roots of the eigenvalues of Christoffel tensor $\mathbf{\Gamma}(\mathbf{n})$.

- If $V_P(\mathbf{n}) \neq V_{S1}(\mathbf{n}) \neq V_{S2}(\mathbf{n})$, the wavefront normal direction \mathbf{n} is non-singular, and equation 40 results in three distinct eigenvectors — the unit polarization vectors $\mathbf{U}^P(\mathbf{n})$, $\mathbf{U}^{S1}(\mathbf{n})$, and $\mathbf{U}^{S2}(\mathbf{n})$. Then equation 4 defines three group-velocity vectors $\mathbf{g}^P(\mathbf{n})$, $\mathbf{g}^{S1}(\mathbf{n})$, and $\mathbf{g}^{S2}(\mathbf{n})$ and three unit ray-direction vectors $\mathbf{r}^P(\mathbf{n})$, $\mathbf{r}^{S1}(\mathbf{n})$, and $\mathbf{r}^{S2}(\mathbf{n})$, the triples of both vectors $\mathbf{g}(\mathbf{n})$ and $\mathbf{r}(\mathbf{n})$ uniquely determined.
- Alternatively, if at least two phase velocities $V_P(\mathbf{n})$, $V_{S1}(\mathbf{n})$, and $V_{S2}(\mathbf{n})$ coincide, the wavefront normal direction \mathbf{n} becomes singular, $\mathbf{n} = \mathbf{n}^s$, generally resulting in an infinite number of polarization vectors \mathbf{U} of body waves corresponding to the singularity. Only at kiss singularities⁹ the uniqueness of vectors $\mathbf{g}(\mathbf{n}^s)$ and $\mathbf{r}(\mathbf{n}^s)$ is maintained despite the nonuniqueness of $\mathbf{U}(\mathbf{n}^s)$. All other singularities produce an infinite number of vectors $\mathbf{g}(\mathbf{n}^s)$ and $\mathbf{r}(\mathbf{n}^s)$.

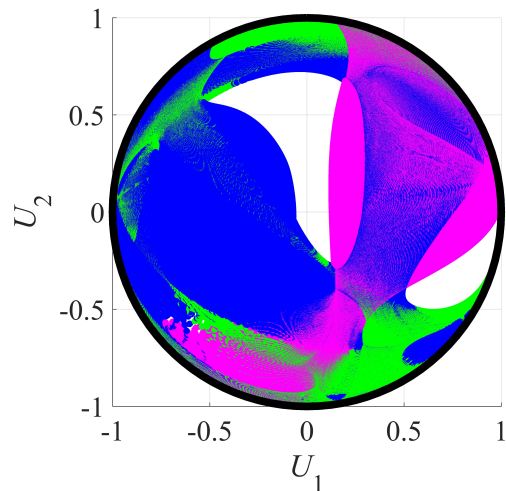


FIG. 7: Projections of polarization vectors \mathbf{U}^P (magenta), \mathbf{U}^{S1} (blue), and \mathbf{U}^{S2} (green) of the P-, fast S_1 -, and slow S_2 -waves, respectively, onto the horizontal plane. The computations are carried out in model 39 for the wavefront normal directions \mathbf{n} , covering the entire unit sphere.

2. Input ray direction \mathbf{r} . Equations 22 in Grechka⁶ or equations 2.C.13 and 2.C.14 in Grechka and Heigl¹⁰ comprise an algebraic system of degree 43 that has an odd number of non-centrally symmetric real-valued solutions $\{\mathbf{n}(\mathbf{r}), \mathbf{U}(\mathbf{r})\}$, ranging from 3 to 19 and representing the uniquely determinable parameters of plane waves propagating along a given ray direction \mathbf{r} . Although the system degenerates at kiss singularities because of the nonuniqueness of $\mathbf{U}(\mathbf{r})$, it yields a unique wavefront normal $\mathbf{n}(\mathbf{r}) = \mathbf{r}$ there.

3. Input polarization vector \mathbf{U} . Equations 1 solved for the slowness vector $\mathbf{p}(\mathbf{U})$ can have from 0 to 4 or infinite number of real-valued solutions and the same number of solutions for the group-velocity vector $\mathbf{g}(\mathbf{p}, \mathbf{U})$.

Clearly, different inputs — \mathbf{n} , \mathbf{r} , or \mathbf{U} — lead to very different descriptions of wave propagation in homogeneous anisotropic media. The knowledge of either the wavefront normal \mathbf{n} or the ray direction \mathbf{r} guarantees the presence of at least three plane body-wave solutions, whereas the specification of polarization vector \mathbf{U} can result in no solutions.

¹ E. B. Christoffel, *Annali di Matematica* **8**, 193 (1877).

² F. I. Fedorov, *Theory of elastic waves in crystals* (Plenum Press, 1968).

³ M. J. P. Musgrave, *Crystal acoustics* (Holden-Day, 1970).

⁴ B. A. Auld, *Acoustic fields and waves in solids* (John Wiley and Sons., 1973).

⁵ V. Červený, *Seismic ray theory* (Cambridge University Press, 2001).

⁶ V. Grechka, *Geophysics* **82**, no. 4, WA45 (2017).

⁷ E. W. Weisstein, *CRC concise encyclopedia of mathematics* (Chapman & Hall/CRC, 2003).

⁸ I. Tsvankin, *Seismic signatures and analysis of reflection data in anisotropic media* (Elsevier, 2001).

⁹ S. Crampin and M. Yedlin, *Journal of Geophysics* **49**, 43 (1981).

¹⁰ V. Grechka and W. M. Heigl, *Microseismic monitoring* (SEG, Geophysical references series, no. 22, 2017).